

A new architecture of planar three-degree-of-freedom parallel manipulator

Clément M. Gosselin[†], Sylvain Lemieux[†] and Jean-Pierre Merlet[‡]

[†]Département de Génie Mécanique, Université Laval
Québec, Québec, Canada, G1K 7P4

[‡]INRIA, Unité de Sophia-Antipolis
B.P. 93, 06902 Sophia-Antipolis, France

Abstract

In this paper, a new architecture of planar three-degree-of-freedom (3-dof) parallel manipulator is presented. In the proposed mechanism, the prismatic actuators are fixed to the base which leads to a reduction of the inertia of the moving links and hence makes it attractive, particularly when high speeds are required and electric actuation is considered. After introducing the mechanism, a kinematic analysis is reported. Then, velocity and acceleration equations are derived. Based on the geometry of the manipulator, a workspace analysis is performed and a description of the boundaries of the workspace is provided. This manipulator can be used in robotic applications involving the positioning and orientation of a rigid body on the plane with high stiffness or accuracy. Additionally, the mechanism can find applications in motion simulators or other high-precision or high-speed devices.

1 Introduction

Parallel mechanical architectures have been originally proposed in the context of tire-testing machines and flight simulators [1]. The main motivation behind the use of such architectures is that they provide better stiffness and accuracy than serial kinematic chains. Moreover, they allow the actuators to be fixed to the base — or to be located close to the base — of the mechanism which minimizes the inertia of the moving parts and which makes it possible to use more powerful actuators. The application of parallel mechanical devices in robotics has been proposed approximately fifteen years ago [2]. Later, extensive studies have led to the identification of several mechanical architectures with potential applications in robotics. Some of these architectures have been analyzed in detail and opti-

mized and some prototypes have been built to demonstrate their properties (see for instance [3–5]). In some instances, it is required to control the motion of a rigid body on a plane with two or three dofs. Examples of applications of planar manipulators include metal cutting, part handling, deburring and simulation devices for terrestrial vehicle simulators. A planar 3-dof parallel manipulator has been proposed in [6], [7]. The kinematic problems associated with this manipulator have been addressed in detail in [8], [7], [9] and [10] and its singularities have been identified in [7]. Efficient algorithms for the determination of its workspace have been proposed in [11]. In all the above references and in other work related to planar 3-dof parallel manipulators, two different architectures have been proposed, i.e., a manipulator with revolute actuators and a manipulator with prismatic actuators. The manipulators consist of three kinematic chains connecting the base to the moving platform. In the case of the manipulator with revolute actuators, each of the chains consists of three consecutive revolute pairs and only the joints fixed to the base are actuated. In the case of the manipulator with prismatic actuators, each of the chains is composed of a passive revolute joint fixed to the base, a moving actuated prismatic joint and a passive revolute joint fixed to the platform.

In this paper, a new architecture of planar 3-dof parallel manipulator is proposed. It departs from the existing designs in that the prismatic actuators are fixed to the base. In other words, each of the chains connecting the base to the platform is composed of a fixed prismatic actuator and two moving passive revolute joints. This architecture is in fact the planar counterpart of the spatial architecture proposed by the same authors in [12]. The positioning and velocity equations of the new planar parallel manipulator are given. Then, a description of the workspace of the manipulator is provided based on the analysis of the

mechanism. Design issues are also addressed, especially in connection with the workspace of the manipulator and examples of possible workspaces are presented. Because of its inherent stiffness and accuracy, and because it allows to reduce the inertia of the moving links, the mechanism studied here can be used in high-performance robotic applications as a planar positioning and orientation device. Moreover, it can also be used in other applications such as vehicle motion simulators, camera positioning devices and other devices which require high-precision or high-bandwidth control. The kinematic, velocity and workspace analyses presented in this paper can be of great help in the design, trajectory planning and control of such devices.

2 Architecture of the new mechanism

The architecture of the proposed planar 3-dof parallel manipulator is illustrated schematically in Fig. 1. A reference frame Oxy is fixed to the base and a moving reference frame $Cx'y'$ is attached to the platform. The three prismatic actuators are fixed to the base. Each of the actuators is located at point A_i (fixed point) and its axis of motion is pointed in a direction defined by angle α_i (fixed angle). Moreover, vector \mathbf{e}_i is defined as a fixed unit vector in the direction of the axis of the i th prismatic actuator. The moving part of the i th actuator is then attached to a second moving link of length l_i by an unactuated revolute joint located at point B_i . The joint coordinate associated with the i th actuator is defined as ρ_i , the distance between points A_i and B_i . Finally, the moving link of length l_i is connected to the platform by a revolute joint located at point C_i . The Cartesian coordinate vector of the manipulator is given by the position and orientation of the platform and can be written as

$$\mathbf{p} = [x_C \ y_C \ \phi]^T \quad (1)$$

where (x_C, y_C) are the position coordinates of point C expressed in the fixed frame, and ϕ is the angle between the x axis of the fixed frame and axis x' of the moving frame, as indicated on the figure. The actuated joint coordinate vector is defined as

$$\boldsymbol{\rho} = [\rho_1 \ \rho_2 \ \rho_3]^T \quad (2)$$

where each of the components are defined above. Finally, angle β_i is defined as the angle between the x axis of the fixed frame and the intermediate link of length l_i .

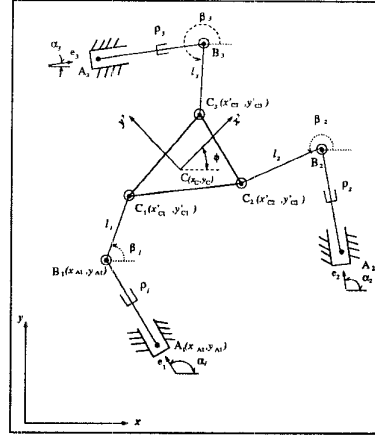


Figure 1: Architecture of the proposed planar 3-dof parallel manipulator.

By controlling the three actuators, it is possible to control the Cartesian coordinates — position and orientation — of the platform, as expected. Moreover, as explained in the introduction, the architecture of each of the kinematic chains connecting the base to the platform is of the PRR type, where P and R respectively denote prismatic and revolute joints. In existing planar 3-dof parallel manipulators, each of the chains connecting the base to the platform are either of the RRR type or of the RPR type. In the latter case, the actuators are prismatic, as for the manipulator proposed here. However, both parts of the prismatic actuators are moving, which increases the inertia. When hydraulic actuators are used, moving actuators are an interesting solution since they lead to very small undesirable transversal forces between the rod and the piston. However, if electrical actuators are used (for instance with a ball screw system), transversal forces are a lot less critical and the design proposed here is of great interest since it reduces the inertia of the moving parts.

3 Kinematic analysis

The most important kinematic issues to be addressed, when considering a new manipulator, are the solutions of the inverse and direct kinematic problems. Following the notation defined above, the geometry of the kinematic chains connecting the base to the platform allows one to write the coordinates of point C_i , noted (x_{C_i}, y_{C_i}) , as

$$x_{C_i} = x_{A_i} + \rho_i \cos \alpha_i + l_i \cos \beta_i, \quad i = 1, 2, 3 \quad (3)$$

$$y_{C_i} = y_{A_i} + \rho_i \sin \alpha_i + l_i \sin \beta_i, \quad i = 1, 2, 3 \quad (4)$$

Moreover, these coordinates can also be written as functions of the Cartesian coordinates of the platform, i.e.,

$$x_{C_i} = x_C + x'_{C_i} \cos \phi - y'_{C_i} \sin \phi, \quad i = 1, 2, 3 \quad (5)$$

$$y_{C_i} = y_C + y'_{C_i} \cos \phi + x'_{C_i} \sin \phi, \quad i = 1, 2, 3 \quad (6)$$

where x'_{C_i} and y'_{C_i} are constant parameters describing the geometry of the platform, i.e., they are the coordinates of point C_i in the coordinate frame attached to the platform.

Eqs.(5) and (6) can then be substituted into eqs.(3) and (4), respectively, which leads to two equations from which angle β_i is easily eliminated. This leads to a quadratic equation in ρ_i which can be solved and finally leads to

$$\rho_i = M_i \pm N_i, \quad i = 1, 2, 3 \quad (7)$$

where

$$M_i = (x_{C_i} - x_{A_i}) \cos \alpha_i + (y_{C_i} - y_{A_i}) \sin \alpha_i \quad (8)$$

$$N_i = \sqrt{l_i^2 - S_i^2} \quad (9)$$

$$S_i = (x_{C_i} - x_{A_i}) \sin \alpha_i + (y_{C_i} - y_{A_i}) \cos \alpha_i \quad (10)$$

and x_{C_i} and y_{C_i} are as defined in eqs.(5) and (6). Eq.(7) provides a closed-form solution to the inverse kinematic problem. Indeed, for a given position and orientation of the platform, the joint coordinates can be computed using this equation. Since two solutions are found for each of the joint coordinates, it is clear that the inverse kinematic problem of this manipulator has 8 different solutions.

The second important problem to be addressed is the direct kinematic problem, which consists in finding the position and orientation of the platform for given values of the joint coordinates. This problem has been solved for the existing planar 3-dof parallel manipulators in [8–10]. It was shown to lead to a polynomial of degree 6 which can have up to 6 real solutions. For the mechanism proposed here, it is very easy to show that the direct kinematic problem is geometrically equivalent to the direct kinematic problem of the existing mechanisms. Hence, a polynomial of degree 6 can also be derived for the new manipulator, for instance, using the formulation presented in [10].

4 Velocity equations

Eq.(7) can be differentiated with respect to time in order to obtain the velocity equations. This leads to an equation of the form

$$\mathbf{A} \dot{\mathbf{p}} + \mathbf{B} \dot{\boldsymbol{\rho}} = \mathbf{0} \quad (11)$$

where $\dot{\mathbf{p}}$ is the vector of Cartesian velocities defined as

$$\dot{\mathbf{p}} = [\dot{x}_C, \dot{y}_C, \dot{\phi}]^T \quad (12)$$

and $\dot{\boldsymbol{\rho}}$ is the vector of joint velocities defined as

$$\dot{\boldsymbol{\rho}} = [\dot{\rho}_1, \dot{\rho}_2, \dot{\rho}_3]^T \quad (13)$$

Matrices \mathbf{A} and \mathbf{B} are the 3×3 Jacobian matrices of the manipulator and can be expressed as

$$\mathbf{A} = \begin{bmatrix} a_1 & b_1 & c_1 \\ a_2 & b_2 & c_2 \\ a_3 & b_3 & c_3 \end{bmatrix} \quad (14)$$

$$\mathbf{B} = \begin{bmatrix} d_1 & 0 & 0 \\ 0 & d_2 & 0 \\ 0 & 0 & d_3 \end{bmatrix} \quad (15)$$

where one has, for $i = 1, 2, 3$,

$$a_i = -\rho_i \cos \alpha_i - x_{A_i} + x_C + x'_{C_i} \cos \phi - y'_{C_i} \sin \phi \quad (16)$$

$$b_i = -y_{A_i} + y_C + y'_{C_i} \cos \phi + x'_{C_i} \sin \phi - \rho_i \sin \alpha_i \quad (17)$$

$$c_i = -x'_{C_i} y_{A_i} \cos \phi + x'_{C_i} y_C \cos \phi + \rho_i y'_{C_i} \cos(\phi - \alpha_i) + x_{A_i} y'_{C_i} \cos \phi - x_C y'_{C_i} \cos \phi + x_{A_i} x'_{C_i} \sin \phi - x_C x'_{C_i} \sin \phi + y_{A_i} y'_{C_i} \sin \phi - y_C y'_{C_i} \sin \phi + \rho_i x'_{C_i} \sin(\phi - \alpha_i) \quad (18)$$

$$d_i = \rho_i + x_{A_i} \cos \alpha_i - x_C \cos \alpha_i - x'_{C_i} \cos(\phi + \alpha_i) + y'_{C_i} \sin(\phi - \alpha_i) + y_{A_i} \sin \alpha_i - y_C \sin \alpha_i \quad (19)$$

Eq.(11) relates the Cartesian velocities of the mechanism to its joint velocities. This relationship is also very important for the description of the different types of singularities of the manipulator. The conditioning of the Jacobian matrices can also be used to characterize the dexterity of the mechanism.

5 Workspace analysis

One of the most important issues to be considered in the design of manipulators is their workspace. For

parallel manipulators, this issue is even more critical since parallel mechanisms may sometimes have a rather limited workspace. The determination of the workspace of parallel manipulators has been addressed, for instance, in [11]. More specifically, the determination of the workspace of planar parallel manipulators has been addressed in [7], [13] and [14]. However, the algorithms presented in the latter references cannot be directly applied to the manipulator introduced here and a new method has to be derived.

The workspace of a planar 3-dof manipulator is often represented as a region of the plane which can be attained by a reference point on the platform, for a given *fixed orientation of the platform*. This representation can be repeated for any orientation of the platform and hence it completely describes the workspace of a 3-dof manipulator. It will therefore be adopted here. The problem of the determination of the workspace of the manipulator introduced here can then be stated as follows: for given geometric parameters of the robot and for a given orientation of the platform (i.e., for a given value of angle ϕ), find the region of the plane which can be attained by point C of the platform (or any other point selected on the platform) without exceeding the mechanical limits of the manipulator. These limits will include here the limits associated with the closed kinematic chains and the motion limits of the prismatic actuators.

Since the region of the plane described above is obtained for a given orientation of the platform, it is clear that it can be defined as the intersection of three regions which are simply the regions that point C can attain — for a constant orientation — when considering the constraints on each of the legs of the manipulator independently. Therefore, the workspace will be obtained as the intersection of three regions. Moreover, each of these three regions can be described by its boundary, as will be shown below, and the intersection of the regions will therefore be obtained using the intersection of the boundaries of the workspace. The general algorithm is similar to what was presented in [11] and can be summarized as follows: *i*) Find the curves defining the boundary of the three regions corresponding to the constraints associated with each of the legs independently, *ii*) Find the intersections of the curves defining the boundary of the three regions (intersections of all the curves with one another), *iii*) Divide the curves in elementary portions — i.e. portions with no intersection with other curves — using the intersections found in the previous step, *iv*) Test each of the elementary portions to determine which ones are part of the envelope of the global workspace.

From Fig. 1, it is clear that the region which can be attained by point C with a constant orientation of the platform and considering the constraints on only one leg will in general be limited by two parallel line segments connected in their ends by two half-circles and with a possible internal void region, as illustrated in Fig. 2. The line segments can be described mathematically as

$$x = x_{Ai} + \rho_{i,min} \cos \alpha_i - (x'_{Ci} \cos \phi - y'_{Ci} \sin \phi) \pm l_i \sin \alpha_i + \lambda_i \cos \alpha_i \quad (20)$$

$$y = y_{Ai} + \rho_{i,min} \sin \alpha_i - (x'_{Ci} \sin \phi + y'_{Ci} \cos \phi) \pm l_i \cos \alpha_i + \lambda_i \sin \alpha_i \quad (21)$$

where λ_i is the parameter of the curves and is bounded by

$$\rho_{i,min} \leq \lambda_i \leq \rho_{i,max} \quad (22)$$

where $\rho_{i,min}$ and $\rho_{i,max}$ are respectively the minimum and maximum possible value of the i th joint variable (constraints). Similarly, the half-circles can also be represented as parametric curves, i.e.,

$$x = x_{Ai} + \rho_{i,min} \cos \alpha_i - (x'_{Ci} \cos \phi - y'_{Ci} \sin \phi) + l_i \cos \psi_i \quad (23)$$

$$y = y_{Ai} + \rho_{i,min} \sin \alpha_i - (x'_{Ci} \sin \phi + y'_{Ci} \cos \phi) + l_i \sin \psi_i \quad (24)$$

with ψ_i the parameter bounded as

$$\alpha_i - \frac{3\pi}{2} \leq \psi_i \leq \alpha_i - \frac{\pi}{2} \quad (25)$$

for the first half-circle and

$$x = x_{Ai} + \rho_{i,max} \cos \alpha_i - (x'_{Ci} \cos \phi - y'_{Ci} \sin \phi) + l_i \cos \psi_i \quad (26)$$

$$y = y_{Ai} + \rho_{i,max} \sin \alpha_i - (x'_{Ci} \sin \phi + y'_{Ci} \cos \phi) + l_i \sin \alpha_i \quad (27)$$

with

$$\alpha_i - \frac{\pi}{2} \leq \psi_i \leq \alpha_i + \frac{\pi}{2} \quad (28)$$

for the second half-circle. Finally, the circular arcs defining the void must be described. The following test is applied in order to determine whether or not these arcs will be present, i.e.,

$$\rho_{i,max} - \rho_{i,min} < 2l_i \quad (29)$$

If this condition is verified, then the arcs will be present and their parametric representation can be

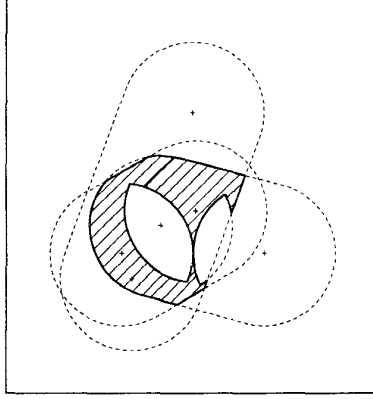


Figure 2: Example of the determination of the workspace.

written as

$$x = x_{Ai} + \rho_{i,min} \cos \alpha_i - (x'_{Ci} \cos \phi - y'_{Ci} \sin \phi) + l_i \cos \varepsilon_i \quad (30)$$

$$y = y_{Ai} + \rho_{i,min} \sin \alpha_i - (x'_{Ci} \sin \phi + y'_{Ci} \cos \phi) + l_i \sin \varepsilon_i \quad (31)$$

for the first arc, where ε_i is the parameter bound by

$$\alpha_i - \arccos(V_i) \leq \varepsilon_i \leq \alpha_i + \arccos(V_i) \quad (32)$$

with

$$V_i = \frac{\rho_{i,max} - \rho_{i,min}}{2l_i} \quad (33)$$

and, for the second arc,

$$x = x_{Ai} + \rho_{i,max} \cos \alpha_i - (x'_{Ci} \cos \phi - y'_{Ci} \sin \phi) + l_i \cos \varepsilon_i \quad (34)$$

$$y = y_{Ai} + \rho_{i,max} \sin \alpha_i - (x'_{Ci} \sin \phi + y'_{Ci} \cos \phi) + l_i \sin \varepsilon_i \quad (35)$$

where ε_i is the parameter bound by

$$\alpha_i - \arccos(V_i) + \pi \leq \varepsilon_i \leq \alpha_i + \arccos(V_i) + \pi \quad (36)$$

With the above expressions, all the portions of curve defining the limits of the region obtained when considering the constraints on one of the legs only are described. Their intersection must then be computed.

Since all the equations are in parametric form and correspond to simple geometric entities (line segments, circular arcs), the computation of the intersections is straightforward. Hence, each of the elements of each of the regions is intersected with all the others. Once all the intersections have been computed, each of the

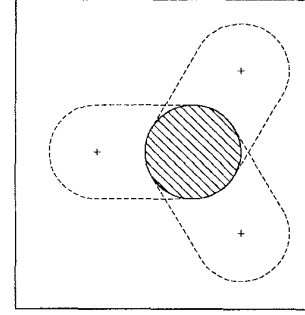


Figure 3: Example of workspace obtained with a symmetric arrangement of the actuators.

curves is considered and the intersections on this element are ordered. Then, the curve is segmented, i.e., divided in elementary portions, where an elementary portion is defined as a portion of the curve which does not intersect any of the other curves. Finally, each of the elementary portions of each of the curves is tested to determine whether or not it is part of the limit of the workspace. The test to be used is straightforward and consists in determining if one point of the curve is inside the two regions — out of the three regions which are intersected — to which the curve does not belong. If the point is inside the other two regions, then this element of curve is part of the boundary of the workspace. All the elements are finally assembled, leading to an exact, compact and efficient description of the workspace. An example of final result is shown in Fig. 2, where the three regions associated with the constraints of the legs are also shown in dotted lines.

6 Examples and design issues

Since the workspace can be easily determined using the algorithm of the preceding section, it is possible to study several designs and to compare their workspace. In general, it will be desirable to maximize the workspace of the manipulator. One immediate possibility is to eliminate the voids in the regions associated with the legs by imposing that

$$\rho_{i,max} - \rho_{i,min} > 2l_i \quad (37)$$

Moreover, the location of the actuators on the base and the geometry of the platform can be modified in order to lead to a larger overlap of the three regions. Examples are shown in Figs. 3 and 4. Other characteristics of the manipulator such as kinematic accuracy, stiffness and dynamic properties must also be consid-

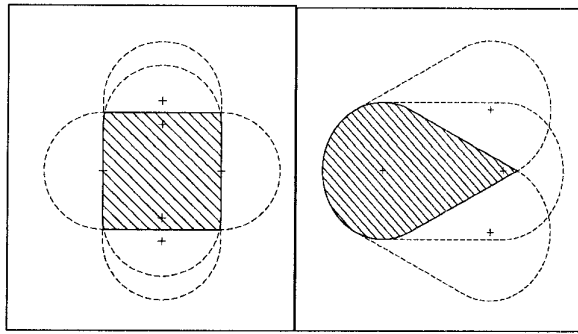


Figure 4: Example of a square workspace and of a workspace obtained with the actuators in close directions.

ered in the design process and are easily mapped onto the workspace.

7 Conclusion

A novel architecture of planar 3-dof parallel manipulator has been proposed and analyzed in this paper. The positioning and velocity equations have been derived. A description of the boundaries of the workspace of the manipulator has also been provided. Because of its inherent stiffness and accuracy, and because it allows to reduce the inertia of the moving links, the mechanism studied here can be used in high-performance robotic applications as a planar positioning and orientation device or in other applications such as vehicle motion simulators. It constitutes an interesting alternative to existing designs, especially when electrical actuation is considered. The kinematic and workspace analyses presented in this paper can be of great help in the design, trajectory planning and control of such devices. Future work includes the development of a prototype of fast positioning device based on the mechanical architecture presented here.

Acknowledgements: This work has been supported by the Natural Sciences and Engineering Research Council of Canada (NSERC), by the Fonds pour la Formation des Chercheurs et l'Aide à la Recherche du Québec (FCAR) and by a France/Québec collaboration grant.

References

[1] D. Stewart, 'A platform with six degrees of freedom', *Proc. of the Inst. of Mech. Eng.*, Vol. 180, No. 5, pp. 371–378, 1965.

[2] H. MacCallion and D.T. Pham, 'The analysis of a six-degree-of-freedom work station for mechanised assembly', *Proc. of the 5th World Congress on TMM*, Montréal, 1979.

[3] E.F. Fichter, 'A Stewart platform-based manipulator: general theory and practical construction', *The Int. J. of Rob. Res.*, Vol. 5, No. 2, pp. 157–182, 1986.

[4] J.-P. Merlet, 'Force-feedback control of parallel manipulators', *Proc. of the IEEE Int. Conf. on Rob. and Auto.*, Vol. 3, pp. 1484–1489, 1988.

[5] C. Gosselin and J.-F. Hamel, 'The agile eye: a high-performance three-degree-of-freedom camera-orienting device', *Proc. of the IEEE Int. Conf. on Rob. and Auto.*, pp. 781–786, 1994.

[6] A.H. Shirkhodaie and A.H. Soni, 'Forward and inverse synthesis for a robot with three degrees of freedom', *Proc. of the Summer Computer Simulation Conference*, Montréal, pp. 851–856, 1987.

[7] C. Gosselin and J. Angeles, 'The optimum kinematic design of a planar three-degree-of-freedom parallel manipulator', *ASME J. of Mech., Trans., and Auto. in Design*, Vol. 110, No. 1, pp. 35–41, 1988.

[8] E. E. Peysah, 'Determination of the position of the member of three-joint and two-joint four member Assur groups with rotational pairs' (in Russian), *Maschinowedenie*, No. 5, pp. 55–61, 1985.

[9] C. Gosselin, J. Sefroui and M. J. Richard, 'Solutions polynomiales au problème de la cinématique directe des manipulateurs parallèles plans à trois degrés de liberté', *Mech. and Mach. Theo.*, Vol. 27, No. 2, pp.107–119, 1992.

[10] K. Wohlhart, 'Direct kinematic solution of the general planar Stewart platform', *Proc. of the Int. Conf. on Comp. Int. Manuf.*, Zakopane, pp. 403–411, 1992.

[11] C. Gosselin, 'Determination of the workspace of 6-DOF parallel manipulators', *ASME J. of Mech. Design*, Vol. 112, No. 3, pp. 331–336, 1990.

[12] J.-P. Merlet and C. Gosselin, 'Nouvelle architecture pour un manipulateur parallèle à six degrés de liberté', *Mech. and Mach. Theo.*, Vol. 26, No. 1, pp. 77–90, 1991.

[13] R.L. Williams and C.F. Reinholtz, 'Closed-form workspace determination and optimization for parallel robotic mechanisms', *Proc. of the ASME Mech. Conf.*, Vol. 3, pp. 341–351, 1988.

[14] G.R. Pennock and D.J. Kassner, 'Kinematic analysis of a planar eight-bar linkage: application to a platform-type robot', *Proc. of the ASME Mech. Conf.*, Vol. DE-25, pp. 37–43, 1990.